Supplement of Earth Surf. Dynam., 7, 723–736, 2019
https://doi.org/10.5194/esurf-7-723-2019-supplement

Earth Surface Dynamics
Open Access
EGU

Supplement of

Seeking enlightenment of fluvial sediment pathways by optically stimulated luminescence signal bleaching of river sediments and deltaic deposits

Elizabeth L. Chamberlain and Jakob Wallinga

Correspondence to: Elizabeth L. Chamberlain (elizabeth.chamberlain@vanderbilt.edu)

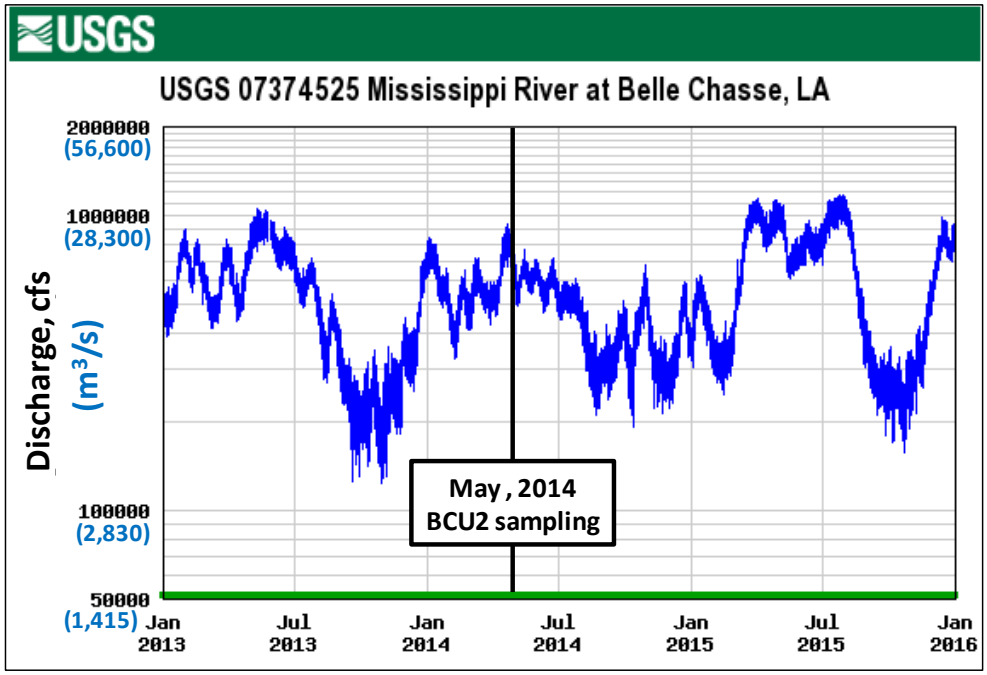

Figure S1. Mississippi River water discharge at Bell Chasse (river km 121), a monitoring station that generally represents discharge conditions at sample site BCU2, for a 3 year interval including the collection date of modern river bedload sand and suspended silt samples. Data obtained from the USGS National Water Information System (waterdata.usgs.gov/nwis/uv?site_no=07374525).

Table S1. Minimum doses ($D_{e,bootMAM}$), central doses ($D_{e,CAM}$), mean doses ($D_{e,MEAN}$), and residual doses for modern river sediments and sands isolated from sedimentary deposits, with (n) accepted aliquots ("al."). Dose rates are given for samples obtained from sedimentary deposits.

Sample name	Lab code	Grain size (μm)	Al. (n)	$D_{e,bootMAM}$ (Gy)	$D_{e,CAM}$ (Gy)	$D_{e,MEAN}$ (Gy)	Residual dose (Gy)	Minimum residual dose (Gy)	Dose rate (Gy/ka)
Modern river suspended load									
BCU2 I-1	LV732	4-20	4	----------	0.028 ± 0.002[a]	0.027 ± 0.001	0.027 ± 0.001	0.026	----------
BCU2 I-2	LV733	4-20	2	----------	0.089 ± 0.021[a]	0.088 ± 0.031	0.088 ± 0.031	0.057	----------
BCU2 I-3	LV734	4-20	3	----------	0.060 ± 0.010[a]	0.040 ± 0.014	0.040 ± 0.014	0.026	----------
BCU2 I-4	LV735	4-20	2	----------	0.099 ± 0.016[a]	0.100 ± 0.022	0.100 ± 0.022	0.078	----------
BCU2 I-5	LV736	4-20	2	----------	0.140 ± 0.010[b]	0.135 ± 0.013	0.135 ± 0.013	0.122	----------
BCU2 I-3	LV734	45-75	---	----------	did not produce a measurable signal				----------
BCU2 I-5	LV734	45-75	4	----------	0.493 ± 0.236[a]	0.227 ± 0.149	0.227 ± 0.149	0.078	----------
Modern river bedload									
BCU2 I-6	LV737	125-180	36	0.027 ± 0.051[b]	1.62 ± 0.29[a]	1.30 ± 0.21	1.62 ± 0.29	1.33	----------
BCU2 I-6	LV737	180-250	30	0.79 ± 0.53[b]	10.5 ± 1.7[a]	10.4 ± 1.5	10.5 ± 1.7	8.8	----------
Lafourche mouth-bar deposits									
GM I-2	LV729	75-125	64	1.99 ± 0.08	2.12 ± 0.06	2.11 ± 0.06	0.13 ± 0.10	0.03	2.34 ± 0.12
BC I-1	LV774	75-125	68	2.94 ± 0.29	3.87 ± 0.16	4.07 ± 0.18	0.93 ± 0.33	0.60	2.18 ± 0.11
CV I-1	LV778	75-125	84	2.69 ± 0.12	2.81 ± 0.04	2.83 ± 0.04	0.12 ± 0.13	-0.01	2.59 ± 0.14
CV II-1	LV780	75-125	82	2.53 ± 0.10	2.66 ± 0.03	2.67 ± 0.04	0.14 ± 0.10	0.04	2.39 ± 0.12
RL I-1	LV724	125-180	54	2.79 ± 0.23	4.36 ± 0.25	4.65 ± 0.27	1.56 ± 0.33	1.23	1.72 ± 0.07
RL I-2	LV725	125-180	58	2.90 ± 0.25	4.03 ± 0.21	4.24 ± 0.25	1.13 ± 0.32	0.81	2.17 ± 0.10
FC I-2	LV726	125-180	29	1.39 ± 0.10	1.47 ± 0.05	1.42 ± 0.07	0.08 ± 0.11	-0.03	1.77 ± 0.07
FC I-1	LV727	125-180	48	1.08 ± 0.21	1.42 ± 0.08	1.38 ± 0.07	0.33 ± 0.23	0.01	1.82 ± 0.07
GM I-1	LV728	125-180	40	2.00 ± 0.09	2.24 ± 0.10	2.25 ± 0.13	0.24 ± 0.14	0.10	2.06 ± 0.09
LR I-1	LV730	125-180	54	2.55 ± 0.12	3.53 ± 0.19	3.74 ± 0.21	0.99 ± 0.22	0.77	1.96 ± 0.08
LR I-2	LV731	125-180	47	2.70 ± 0.29	5.88 ± 0.56	7.14 ± 0.69	3.18 ± 0.63	2.55	2.29 ± 0.11
SC I-1	LV771	125-180	30	3.41 ± 0.24	5.14 ± 0.44	5.66 ± 0.56	1.73 ± 0.50	1.23	2.29 ± 0.11
BC I-2	LV773	125-180	53	3.32 ± 0.16	4.07 ± 0.14	4.18 ± 0.15	0.75 ± 0.21	0.54	2.22 ± 0.11
CD I-2	LV776	125-180	59	2.04 ± 0.07	2.09 ± 0.04	2.06 ± 0.05	0.05 ± 0.08	-0.03	2.17 ± 0.10
CD I-1	LV777	125-180	71	1.81 ± 0.13	2.02 ± 0.04	2.04 ± 0.04	0.21 ± 0.13	0.08	2.00 ± 0.08
DL I-2	LV800	125-180	69	2.34 ± 0.06	2.36 ± 0.03	2.38 ± 0.03	0.02 ± 0.07	-0.05	2.18 ± 0.10
DL I-1	LV801	125-180	72	2.37 ± 0.09	2.42 ± 0.03	2.43 ± 0.03	0.05 ± 0.10	-0.05	2.29 ± 0.12

Table S1. Continued.

Lafourche overbank deposits									
EF II-2	LV598	75-125	11	2.76 ± 0.14	2.73 ± 0.21	2.86 ± 0.13	-0.03 ± 0.25	-0.28	3.01 ± 0.19
EF II-3	LV599	75-125	25	3.22 ± 0.11	3.28 ± 0.08	3.08 ± 0.11	0.06 ± 0.14	-0.08	2.41 ±0.13
NV II-4a	LV653	75-125	37	2.54 ± 0.15	2.82 ± 0.13	2.87 ± 0.14	0.28 ± 0.20	0.08	2.39 ± 0.13
NV X-3	LV471	75-125	27	3.64 ± 0.15	4.80 ± 0.34	5.25 ± 0.41	1.16 ± 0.37	0.79	3.13 ± 0.18
EF II-1	LV596	75-125	13	1.91 ± 0.23	1.98 ± 0.12	2.14 ± 0.12	0.07 ± 0.26	-0.19	3.03 ± 0.20
EF II-6	LV721	75-125	34	2.81 ± 0.08	2.82 ± 0.07	2.83 ± 0.08	0.01 ± 0.10	-0.09	2.44 ± 0.13
EF III-1a	LV654	75-125	51	2.58 ± 0.23	3.66 ± 0.16	3.79 ± 0.17	1.08 ± 0.28	0.80	2.63 ± 0.15
NV II-2	LV641	90-180	51	2.75 ± 0.11	2.79 ± 0.07	2.82 ± 0.08	0.05 ± 0.13	-0.08	2.41 ± 0.13
NV II-3	LV642	90-180	50	2.63 ± 0.08	2.64 ± 0.07	2.64 ± 0.07	0.02 ± 0.10	-0.08	2.49 ± 0.14
PV I-7	LV587	90-180	34	2.31 ± 0.05	2.32 ± 0.05	2.33 ± 0.05	0.01 ± 0.07	-0.06	2.50 ± 0.13
PV I-8	LV646	90-180	31	3.41 ± 0.20	5.02 ± 0.36	5.34 ± 0.40	1.61 ± 0.41	1.20	2.54 ± 0.15
NV VIII-1	LV416	75-180	51	1.90 ± 0.07	1.97 ± 0.05	2.02 ± 0.06	0.07 ± 0.09	-0.02	2.72 ± 0.18
NV X-1	LV419	75-180	53	3.82 ± 0.19	4.23 ± 0.14	4.40 ± 0.17	0.48 ± 0.24	0.24	2.49 ± 0.14
NV III-1	LV432	75-180	47	1.69 ± 0.13	1.91 ± 0.07	1.96 ± 0.07	0.22 ± 0.14	0.08	2.60 ± 0.16
NV III-3	LV433	75-180	56	2.68 ± 0.06	2.68 ± 0.05	2.69 ± 0.05	0.01 ± 0.07	-0.06	2.37 ± 0.13
NV IV-1	LV427	75-180	31	1.78 ± 0.21	2.11 ± 0.10	2.17 ± 0.11	0.33 ± 0.24	0.09	2.53 ± 0.16
NV IV-2	LV428	75-180	61	2.04 ± 0.11	2.13 ± 0.04	2.16 ± 0.05	0.08 ± 0.12	-0.04	2.63 ± 0.17
NV V-1	LV435	75-180	44	2.39 ± 0.15	3.06 ± 0.14	3.19 ± 0.15	0.67 ± 0.21	0.46	3.42 ± 0.30
NV V-2	LV436	75-180	42	2.39 ± 0.09	2.89 ± 0.11	3.00 ± 0.13	0.50 ± 0.14	0.36	2.63 ± 0.16
NV VII-1	LV415	75-180	49	2.23 ± 0.08	2.28 ± 0.06	2.35 ± 0.07	0.05 ± 0.10	-0.05	2.69 ± 0.17
NV IX-1	LV418	75-180	68	2.38 ± 0.11	2.54 ± 0.06	2.51 ± 0.06	0.16 ± 0.13	0.03	2.45 ± 0.14
PV I-4	LV287	100-200	31	2.47 ± 0.25	3.14 ± 0.15	3.23 ± 0.15	0.67 ± 0.29	0.38	2.50 ± 0.22
PV I-5	LV288	100-200	45	2.95 ± 0.25	3.52 ± 0.12	3.60 ± 0.12	0.57 ± 0.27	0.30	2.75 ± 0.18

[a]unlogged versions of the age models were used
[b]the unlogged version of the age model didn't work

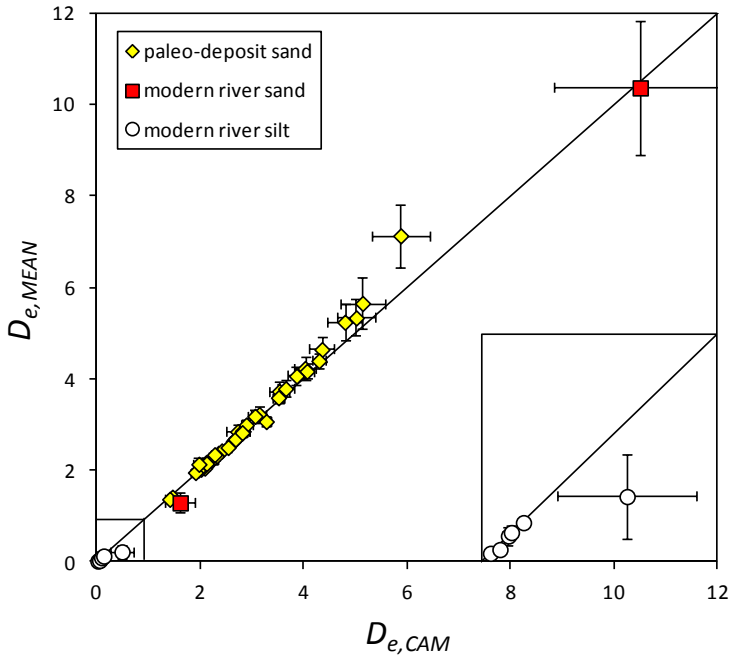

Figure S2. A comparison of $D_{e,CAM}$ and $D_{e,MEAN}$ shows that the two yield similar values for most samples. The inset shows data points within the dose range of 0 - 0.8 Gy.

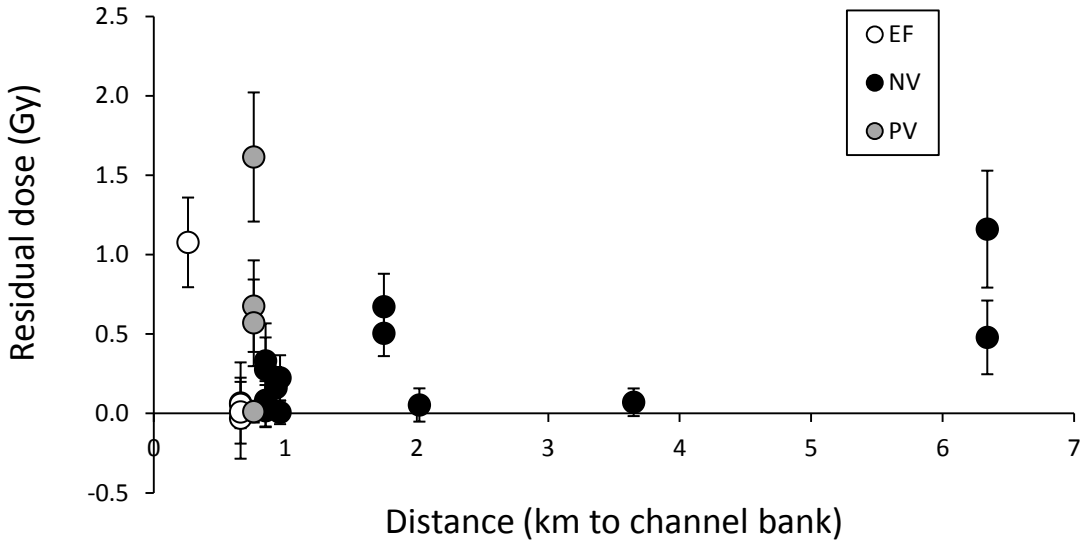

Figure S3. No spatial trend in bleaching was observed in overbank sands sampled at the Elmfield (EF), Napoleonville (NV) and Paincourtville (PV) sites, relative to distance from the channel bank of Bayou Lafourche.

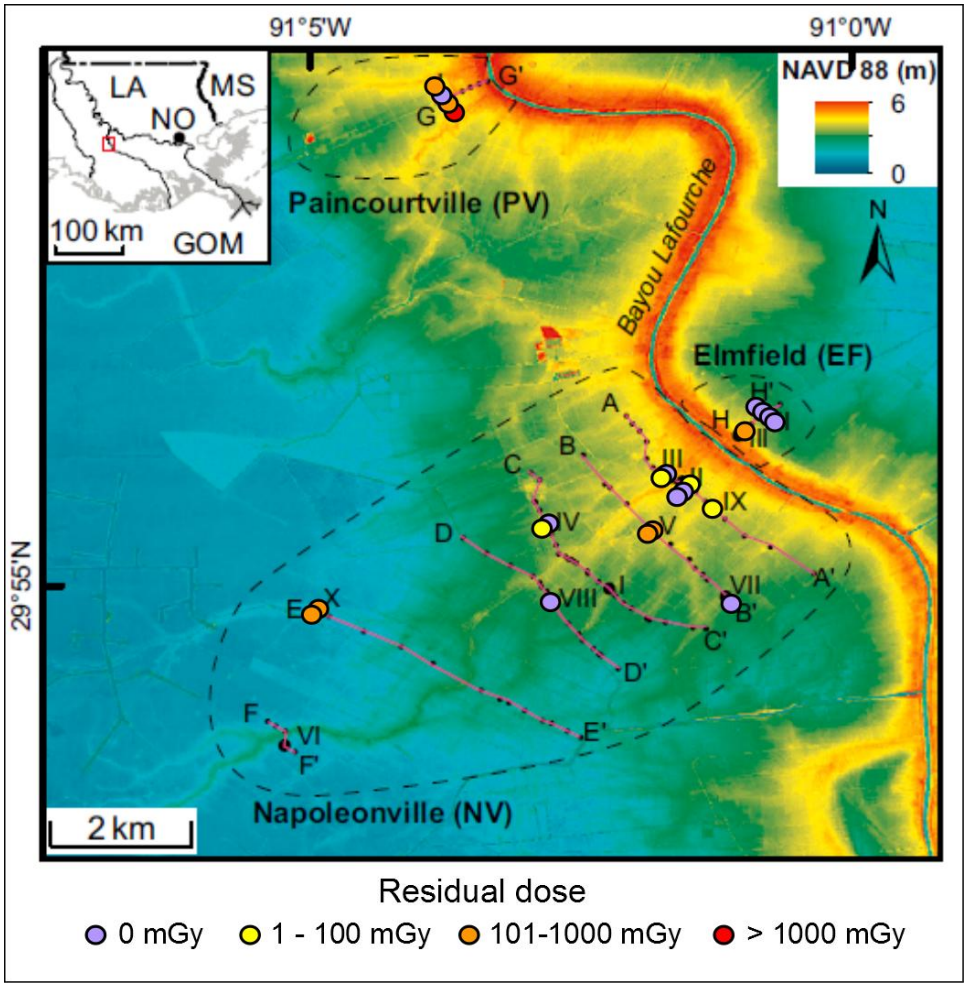

Figure S4. Details of the spatial distribution of overbank sand residual doses. The base map is modified from Shen et al. (2015). Samples from within the same borehole are indicated by stacked (overlapping) symbols, with the deepest sample at the base of the stack (most obscured symbol) and the shallowest sample at the top (most visible symbol). The orientation of the stacks is not meaningful.

Table S2. Details of samples used for the paired sand and silt comparison. See Table S1 for sand dose rates and equivalent doses.

Sample name	Lab code	Silt $D_{e,MEAN}$ (Gy)	Silt $D_{e,CAM}$ (Gy)	Silt dose rate (Gy/ka)	Silt mean age (ka)	Sand bootMAM age (ka)	Sand CAM age (ka)
PV I-4	LV287	3.94 ± 0.25	4.01 ± 0.22	2.78 ± 0.13	1.41 ± 0.11	0.99 ± 0.13	1.26 ± 0.12
PV I-5	LV288	5.28 ± 0.13	5.14 ± 0.13	3.11 ± 0.16	1.70 ± 0.10	1.07 ± 0.11	1.28 ± 0.10
NV II-3	LV642	3.09 ± 0.03	3.11 ± 0.03	2.80 ± 0.13	1.10 ± 0.05	1.06 ± 0.07	1.06 ± 0.06
NV VIII-1	LV416	1.93 ± 0.03	1.95 ± 0.02	3.05 ± 0.14	0.63 ± 0.03	0.70 ± 0.05	0.72 ± 0.05
NV X-1	LV419	3.70 ± 0.06	3.73 ± 0.05	2.80 ± 0.12	1.32 ± 0.06	1.53 ± 0.11	1.73 ± 0.11
EF II-2	LV598	2.50 ± 0.04	2.50 ± 0.05	3.41 ± 0.15	0.73 ± 0.04	0.92 ± 0.07	0.91 ± 0.09
EF II-3	LV599	3.72 ± 0.06	3.71 ± 0.06	2.72 ± 0.11	1.37 ± 0.06	1.33 ± 0.08	1.36 ± 0.08

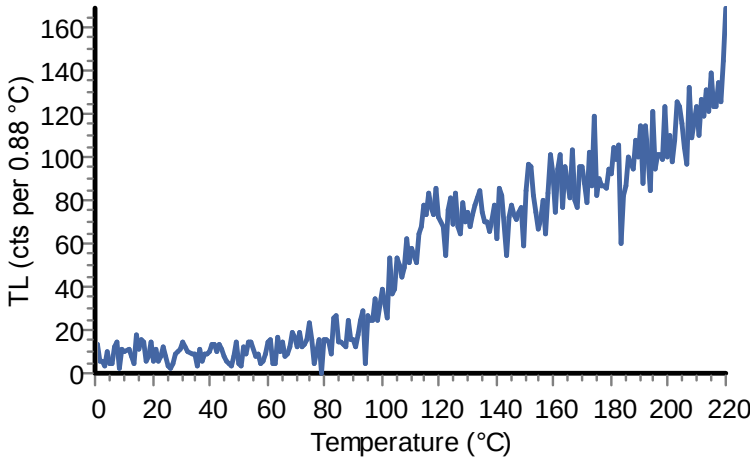

Figure S5. The typical TL response for PV I-4 silt does not show a 110 °C peak, rather the TL signal increases beyond 110 °C suggesting feldspar contamination. Furthermore, PV I-4 and PV I-5 had 20% and 17% of aliquots, respectively, rejected from our analysis for poor reproducibility despite strong luminescence signals. One additional aliquot (5%) of PV I-4 and 4 additional aliquots (13%) of PV I-5 were rejected from our analysis for not meeting infrared (IR) depletion criteria (Duller, 2003), indicating that etching may not have been entirely effective at removing feldspars for these two samples. The finding that no aliquots of the other five samples, that produced agreeing sand/silt ages, were rejected for IR depletion corroborates our suggestion that age overestimation observed for silt samples PV I-4 and 5 is caused by feldspar contamination.

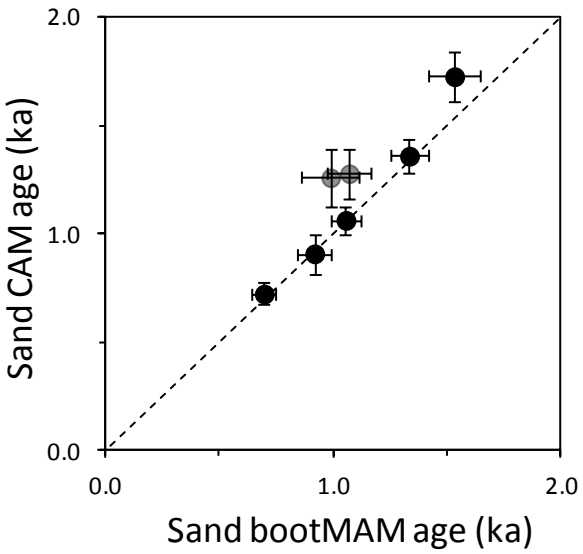

Figure S6. Comparison of sand ages obtained with CAM and bootMAM for the 7 samples used in the paired sand-silt analysis. Gray circles indicate PV I-4 and PV I-5, two samples possibly affected by feldspar contamination in the silt fraction or containing poorly bleached silt.